

Electronic Supporting Information for

Tuning the target composition of amine-grafted CPO-27-Mg for capture of CO₂ in post-combustion and air filtering conditions: a combined experimental and computational study

Maria C. Bernini, Andrés García-Blanco, Jhonny Villarroel-Rocha, David Fairen-Jimenez, Karim Sapag, Antonio J. Ramirez-Pastor and Griselda E. Narda

Section S1. Post-Synthesis Procedure	1
Section S2. Elemental Analysis Results	3
Section S3. Thermal Analysis	3
Section S4. Fourier Transform Infrared Spectroscopy (FTIR).....	6
Section S5. Powder X-Ray Diffraction	7
Section S6. Adsorption Isotherms and Textural Properties.....	8
Section S7. Pore architecture of functionalized models	10
Section S8. Force field and models information.....	13

Section S1. Post-Synthesis Procedure

CPO-27-a: 200 mg of CPO-27 were put in a sealed glass tube connected to a vacuum pump. It was heated in dynamic vacuum conditions at 250 °C during 2 h. The heating rate was controlled at 1 °C min⁻¹ while the cooling rate was set at -5 °C min⁻¹ up to 100 °C. At this temperature, the glass tube was removed from the oven and left at atmospheric conditions, but keeping the vacuum pump working. Once the system was at room temperature, the vacuum was removed and the mass variation was immediately determined ($\Delta m = -33.6\%$). Following, the sample was soaked in a solution of ethylenediamine (6×10^{-3} mmol) in 50 mL of toluene and stirred at room temperature for 65 h. After that, the sample was separated by centrifugation, washed with toluene (2×10 mL) and hexane (1×10 mL), and was dried at 60 °C during two hours. The as-prepared sample was kept in an eppendorf tube at room temperature until usage. Elemental analysis results are shown in Table S1.

CPO-27-b: this sample was obtained by a similar procedure as described for **CPO-27-a**, but the initial weight of the CPO-27 sample was 213 mg. It was heated for 3 h at 250 °C in dynamic vacuum, keeping the heating and cooling rates as in the **CPO-27-a** experiment. The mass variation was determined as $\Delta m = -40\%$. The sample was soaked in a solution of ethylenediamine (10.5 mmol) in 50 mL of toluene. The rest of the procedure was performed as was described for **CPO-27-a** and **CPO-27-b**. Elemental analysis results are shown in Table S1.

CPO-27-c: this sample was obtained by a similar procedure as described for **CPO-27-b**, but the initial weight of the CPO-27 sample was 165 mg. The mass variation was determined as $\Delta m = -35.5\%$. The sample was soaked in a solution of ethylenediamine (7.3 mmol) in 50 mL of toluene. The rest of the procedure was performed as was described for **CPO-27-b**. Elemental analysis results are shown in Table S1.

CPO-27-c': this sample was employed to perform CO₂ and N₂ adsorption isotherms at 323 K, Ar adsorption-desorption isotherm at 77 K, CO₂ recycling experiments at 298 K and CO₂ adsorption microcalorimetry experiments and was obtained by a similar procedure as described for **CPO-27-Mg-c** but using an initial weight sample of 500.6 mg. The mass variation was determined as $\Delta m = -33.74\%$ and the sample was soaked in a solution of ethylenediamine (21.9 mmol) in 50 mL of toluene. The rest of the procedure was performed as was described for **CPO-27-b**. Elemental analysis results are shown in Table S1.

Section S2. Elemental Analysis Results

Table S1. Proposed formulae for the as-prepared and recovered samples from the adsorption isotherms measurements

Sample	Formulae ¹	Elemental Analysis	Formulae ²	Elemental Analysis
CPO-27	$[\text{Mg}_2(\text{DHT})(\text{H}_2\text{O})_2] \cdot 7\text{H}_2\text{O}$	%C: 23.70 Calc. 23.72 %H: 4.97 Calc. 4.94		
CPO-27-a	$[\text{Mg}_2(\text{DHT})(\text{H}_2\text{O})_{1.7}(\text{en})_{0.3}] \cdot 5\text{H}_2\text{O}$	%C: 26.73 Calc. 26.1 %H: 4.29 Calc. 4.67 %N: 2.29 Calc. 2.20	$[\text{Mg}_2(\text{DHT})(\text{H}_2\text{O})_{1.7}(\text{en})_{0.3}] \cdot 3\text{H}_2\text{O}$	%C: 34.36 Calc. 35.46 %H: 3.14 Calc. 2.68 %N: 3.14 Calc. 2.89
CPO-27-b	$[\text{Mg}_2(\text{DHT})(\text{H}_2\text{O})(\text{en})] \cdot 0.2(\text{en}) \cdot 3\text{H}_2\text{O}$	%C: 32.26 Calc. 32.28 %H: 5.17 Calc. 5.07 %N: 8.55 Calc. 8.69	$[\text{Mg}_2(\text{DHT})(\text{H}_2\text{O})_{1.2}(\text{en})_{0.8}] \cdot 0.4\text{CO}_2 \cdot 4\text{H}_2\text{O}$	%C: 29.75 Calc. 29.86 % H: 4.19 Calc. 4.68 % N: 5.99 Calc. 5.57
CPO-27-c	$[\text{Mg}_2(\text{DHT})(\text{H}_2\text{O})_{0.8}(\text{en})_{1.2}] \cdot 0.2(\text{en}) \cdot 3\text{H}_2\text{O}$	%C: 31.88 Calc. 31.38 % H: 5.01 Calc. 5.52 % N: 9.12 Calc. 9.49	$[\text{Mg}_2(\text{DHT})(\text{H}_2\text{O})(\text{en})] \cdot \text{CO}_2 \cdot 2\text{H}_2\text{O}$	%C: 31.82 Calc. 32.95 % H: 4.13 Calc. 4.49 % N: 6.74 Calc. 6.99
CPO-27-c'	$[\text{Mg}_2(\text{DHT})(\text{H}_2\text{O})(\text{en})] \cdot 0.3(\text{en}) \cdot 2\text{H}_2\text{O}$	%C: 34.72 Calc. 33.94 %H: 5.04 Calc. 4.91 %N: 9.66 Calc. 9.72	$[\text{Mg}_2(\text{DHT})(\text{H}_2\text{O})(\text{en})] \cdot \text{CO}_2 \cdot 2\text{H}_2\text{O}$	%C: 33.49 Calc. 32.95 % H: 4.74 Calc. 4.49 % N: 6.65 Calc. 6.99

¹ This formulae correspond to the as-prepared samples. ² This formulae correspond to the evacuated samples recovered after carry out the CO₂ adsorption isotherms

Section S3. Thermal Analysis

The thermogravimetric curves for the CPO-27-Mg and functionalized-CPO-27-Mg samples are shown in Figure S1, while the corresponding DSC curves are displayed in Figure S2. The formulae proposed by the elemental analysis results corresponding to the as-prepared samples¹, have been confirmed by the thermogravimetric analysis. Following the TGA-DSC curves are explained in terms of the process involved in the thermal treatment.

CPO-27-Mg exhibits a first weight loss of 32.08% corresponding to the evacuation of the hydration water molecules (calculated value 31.14%); this process is associated with an endothermic peak in the DSC curve, that is centered at 134 °C. A second mass decay in the TGA curve, corresponding to 9.5%, is related with the loss of the coordinated water molecules (calculated value 8.9%) and is evidenced in the DSC curve as an exothermic peak. The whole decomposition process to render MgO involves a weight loss of 79.6%

and it is in very good agreement with the expected value of 80.09%. This process is denoted in the DSC curve by a strong exothermic signal centered at 474 °C.

CPO-27-Mg-a exhibits a first weight loss of 23.7% corresponding to the evacuation of the hydration water molecules (calculated value 23.6%); this process is associated with a weak and wide endothermic peak in the DSC curve centered at 108 °C. A second mass decay in the TGA curve of 5.7%, is associated with the loss of the coordinated water molecules (calculated value 4.72%); this process is evidenced in the DSC curve by an exothermic peak centered at 231 °C. A third weight loss of 7.6% in the TGA curve occurs between 278-430 °C and can be associated with the evacuation of the coordinated ethylenediamine molecules (calculated value 8.03%). This process is evidenced by an exothermic peak in the DSC curve, centered at 360 °C.

The weight loss for the whole decomposition process of 78.4% is in very good agreement with the expected value of 78.85%.

CPO-27-Mg-b exhibits a first weight loss of 16.64% corresponding to the evacuation of the hydration water molecules and non-coordinated ethylenediamine molecules (calculated value 17.07%); this process is associated with an endothermic peak in the DSC curve centered at 89 °C. A second mass decay in the TGA curve of 5.63%, is associated with the loss of the coordinated water molecule (calculated value 4.65%); being this process evidenced in the DSC curve as an exothermic peak centered at 230 °C. A third weight loss of 14.93% in the TGA curve occurs between 252-440 °C and is related with the elimination of the coordinated ethylenediamine molecules, being the expected value for this step of 15.4%. This process is also evidenced by an exothermic peak in the DSC curve, centered at 347 °C.

The weight loss for the whole decomposition process of 80.5% is in very good agreement with the expected value of 79.15%; this is denoted in the DSC curve by a strong exothermic peak centered at 493 °C.

CPO-27-Mg-c presents a first weight loss of 17.14% corresponding to the evacuation of the hydration water molecules and non-coordinated ethylenediamine molecules (calculated value 16.71%); this process is associated with an endothermic peak in the DSC curve centered at 88 °C. A second mass decay in the TGA curve of 3.46%, is associated with the loss of the coordinated water molecule (calculated value 3.64%); being this process evidenced in the DSC curve as an exothermic peak centered at 228 °C. A third weight loss of 16.56% in the TGA curve occurs between 228-430 °C and is related with the elimination of the coordinated ethylenediamine molecules, being the expected value for this step of 15.25%. This process is also evidenced by an exothermic peak in the DSC curve, centered at 350 °C.

The whole decomposition process involves a mass decay of 80.5% (calculated value 79.59%) and is evidenced in the DSC curve by a strong exothermic peak centered at 504 °C.

In general, the influence of the post-synthesis modification procedure is evidenced in a diminution in the evacuation temperatures of the remaining non-coordinated and coordinated solvent molecules, which is probably due to the weakening produced by the thermal activation followed by the ethylenediamine grafting process. The functionalization seems to increase the thermal stability of the MOF framework since the corresponding decomposition temperatures for the functionalized samples are higher than that of the bare material.

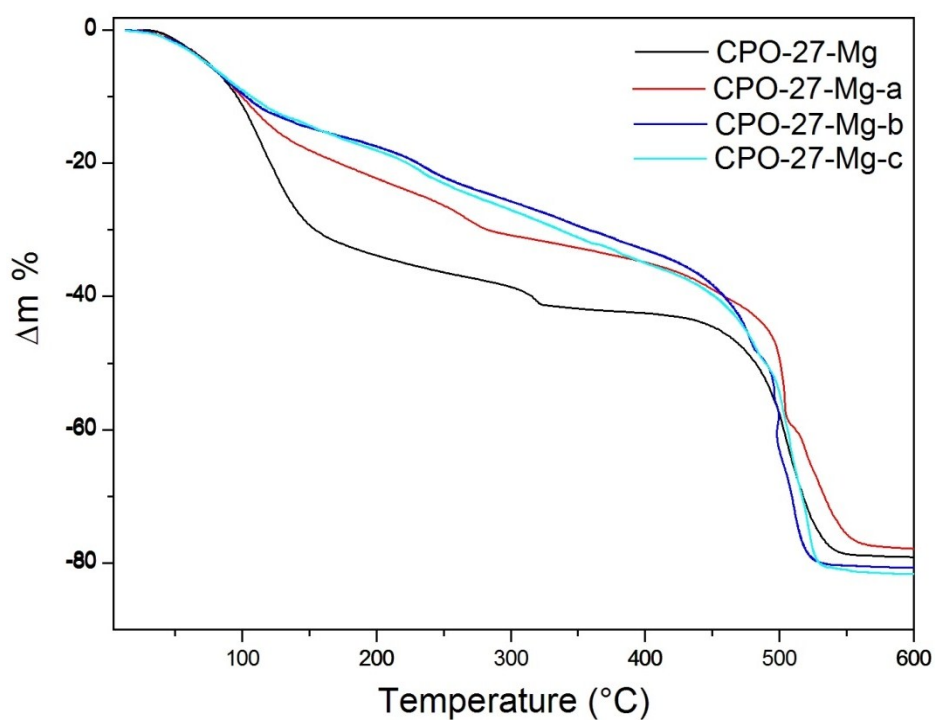


Figure S1. Thermogravimetric curves of CPO-27-Mg, CPO-27-Mg-a, CPO-27-Mg-b, and CPO-27-Mg-c samples.

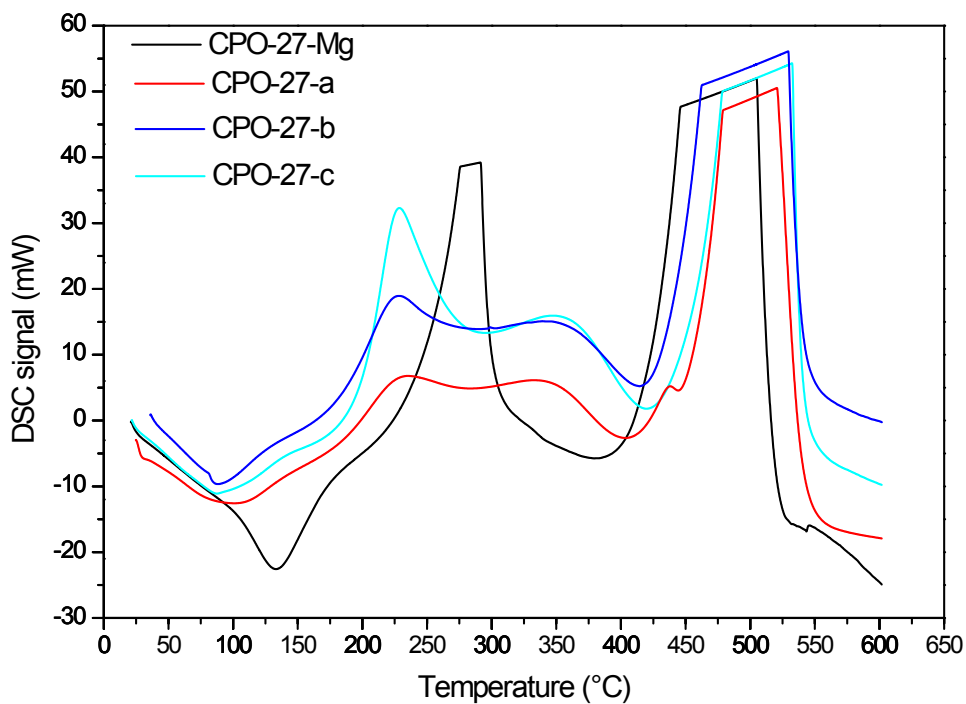


Figure S2. Differential scanning calorimetry (DSC) curves of CPO-27-Mg, CPO-27-Mg-a, CPO-27-Mg-b, and CPO-27-Mg-c samples.

Section S4. Fourier Transform Infrared Spectroscopy (FTIR)

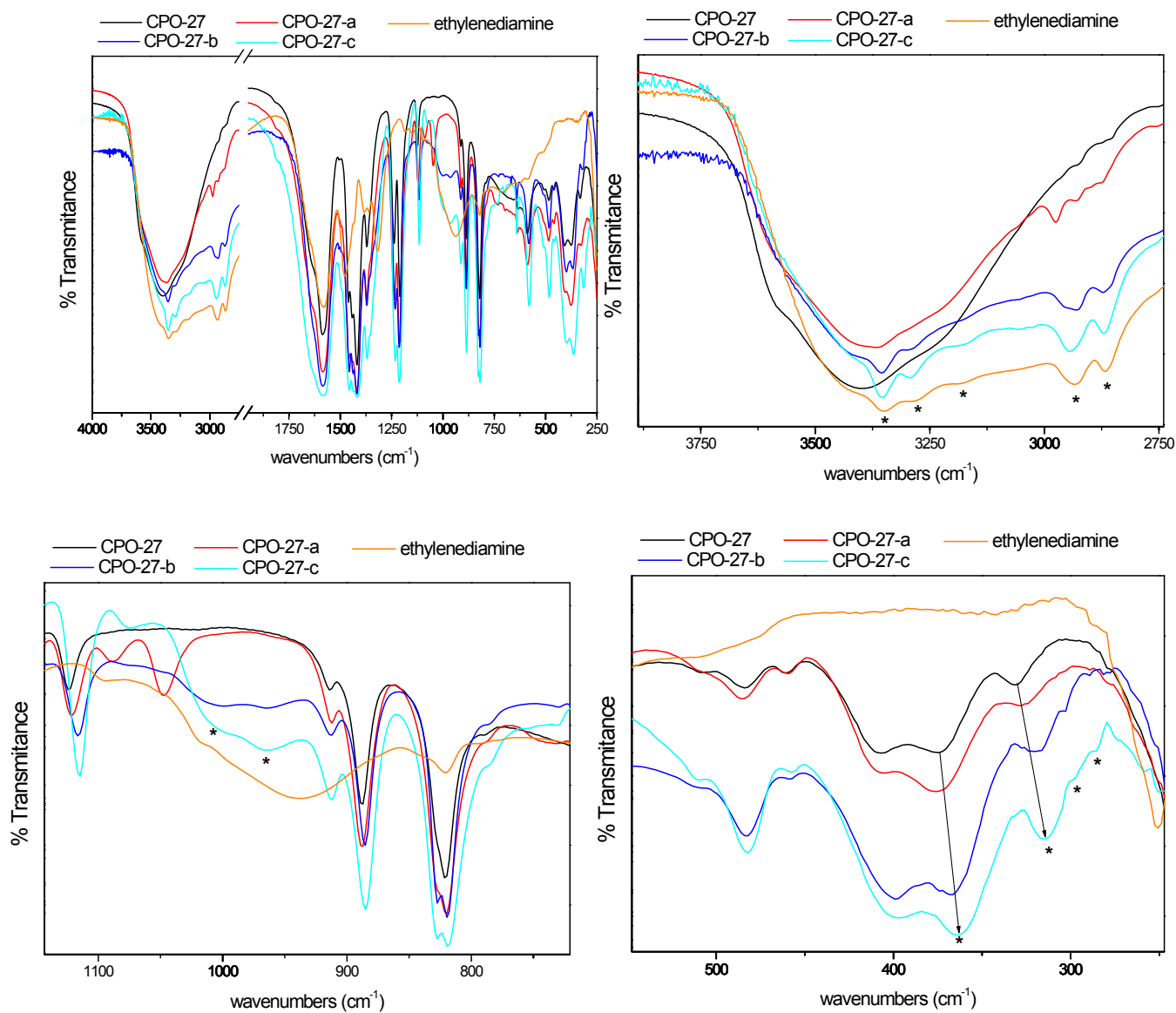


Figure S3. FTIR spectra of CPO-27-Mg and CPO-27-Mg-a, -b and -c samples. Bands marked with * are assigned to vibrations of the ethylenediamine-grated molecules.

Section S5. Powder X-Ray Diffraction

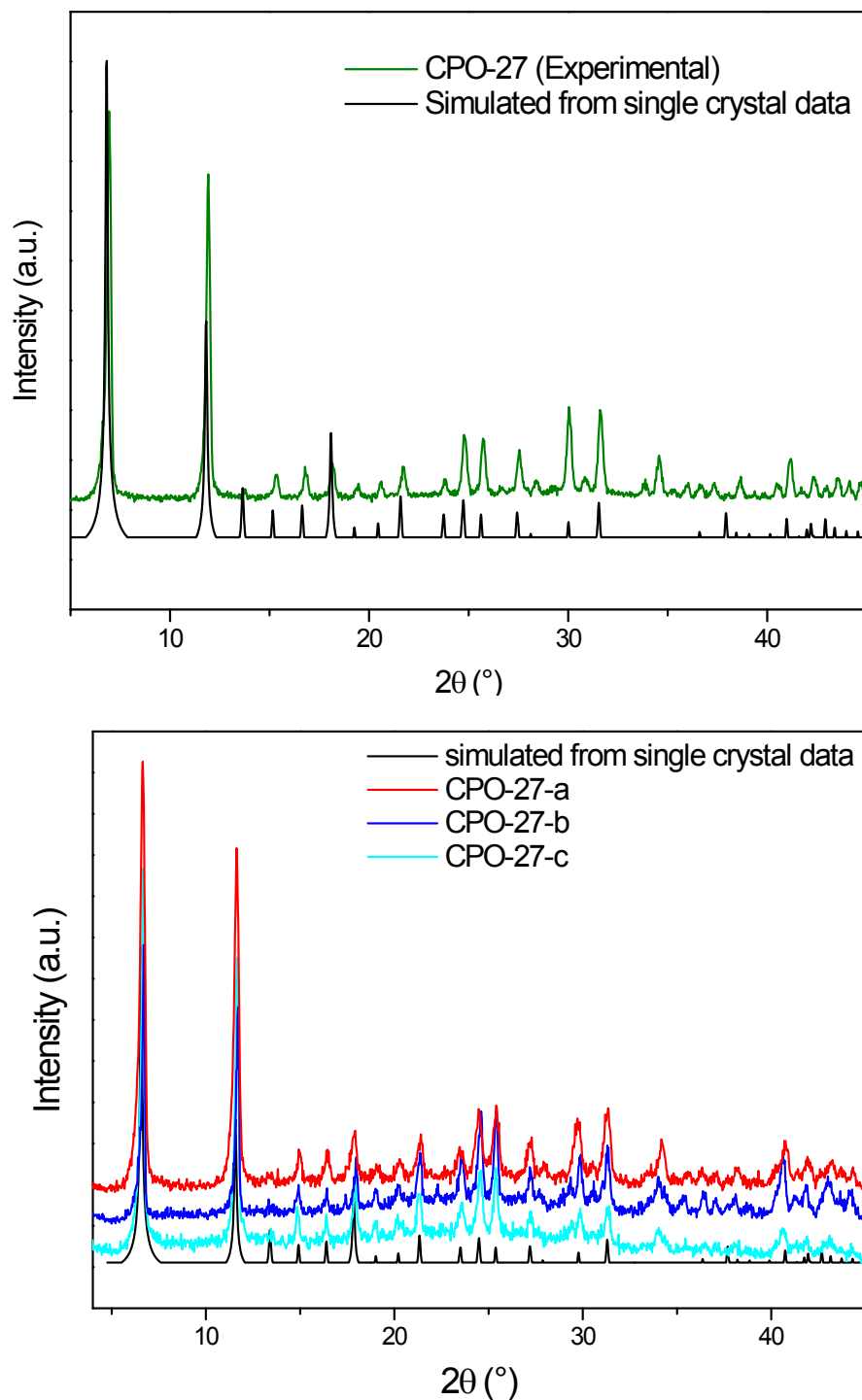


Figure S4. Powder X-ray Diffraction Patterns of CPO-27-Mg (up) and CPO-27-Mg-a, CPO-27-b, and CPO-27-c (down) compared with the corresponding simulated pattern from the cif database available in RASPA code¹.

Section S6. Adsorption Isotherms and Textural Properties

Experimental details of CO₂ and N₂ adsorption recyclings

Previously to obtain the isotherms, the CPO-27-Mg samples were degassed at 523 K (or 503 K in the case of ethylenediamine grafted samples) during 6 h in dynamic vacuum (20 μ Torr).

After the outgassing step, the **CPO-27-Mg-c** CO₂ adsorption-desorption isotherms were obtained at 298 K. Subsequently, the sample was outgassed again, in the measurement port, in the same conditions as previously described. A second CO₂ adsorption isotherm was collected immediately.

An analogous procedure was applied to the non-functionalized material.

To evaluate the stability of the porosity of both materials under the recycling conditions, an equivalent experiment was performed by adsorbing N₂ at 77 K in two consecutive cycles. All of these experiments were carried out in a manometric adsorption apparatus (Micromeritics, ASAP 2050).

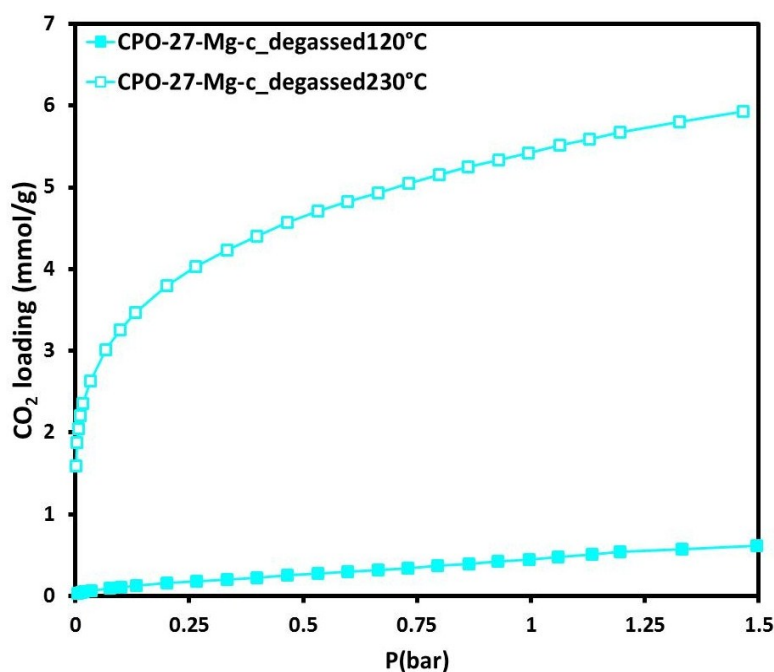


Figure S5. CO₂ adsorption isotherms of CPO-27-Mg-c outgassed at 120 °C (blue) and 230 °C (red).

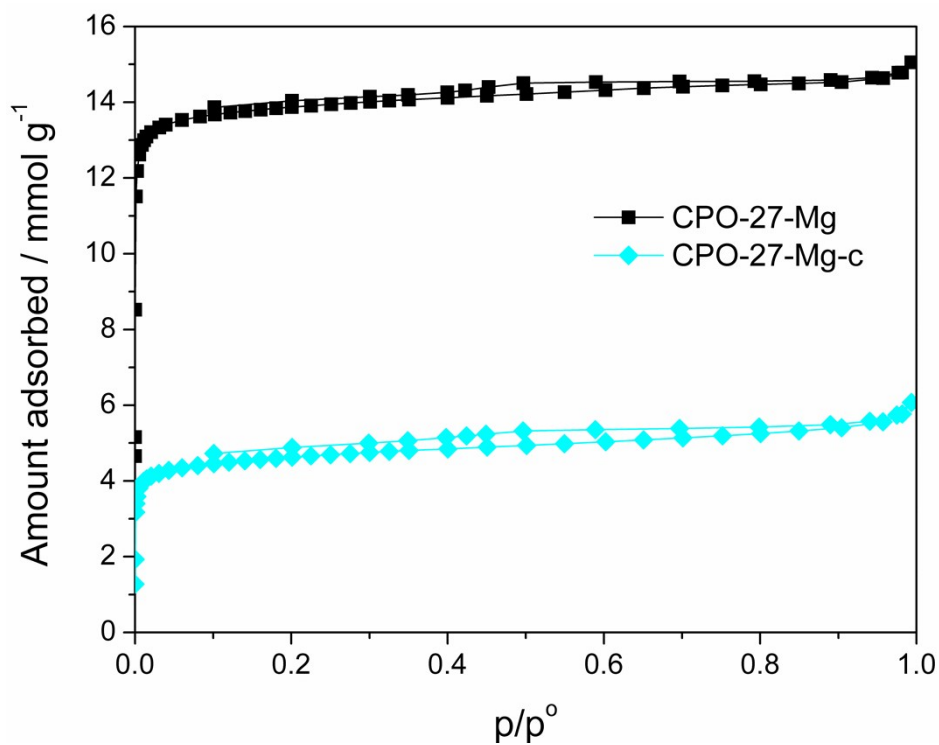


Figure S6. N₂ adsorption-desorption isotherms at 77 K of CPO-27-Mg (black squares) and CPO-27-Mg-c (cyan rhomboids).

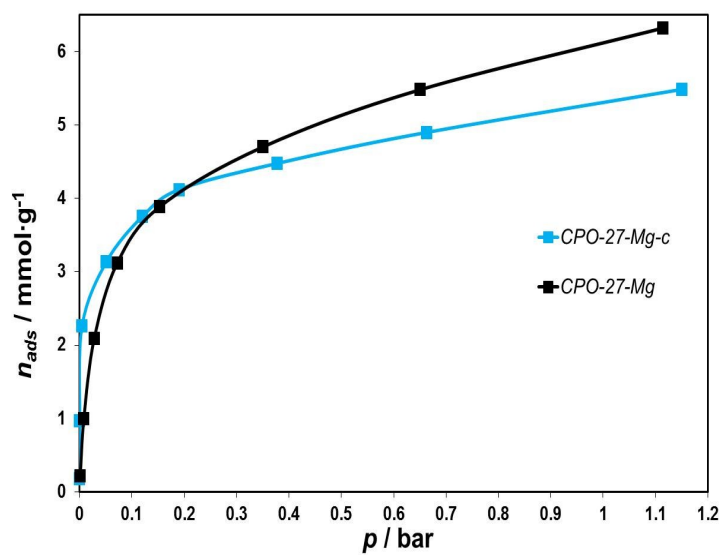


Figure S7. CO₂ adsorption isotherms of CPO-27-Mg and CPO-27-Mg-c samples obtained during the microcalorimetric experiments at 296 K.

Section S7. Pore architecture of functionalized ethylenediamine@CPO-27-Mg models

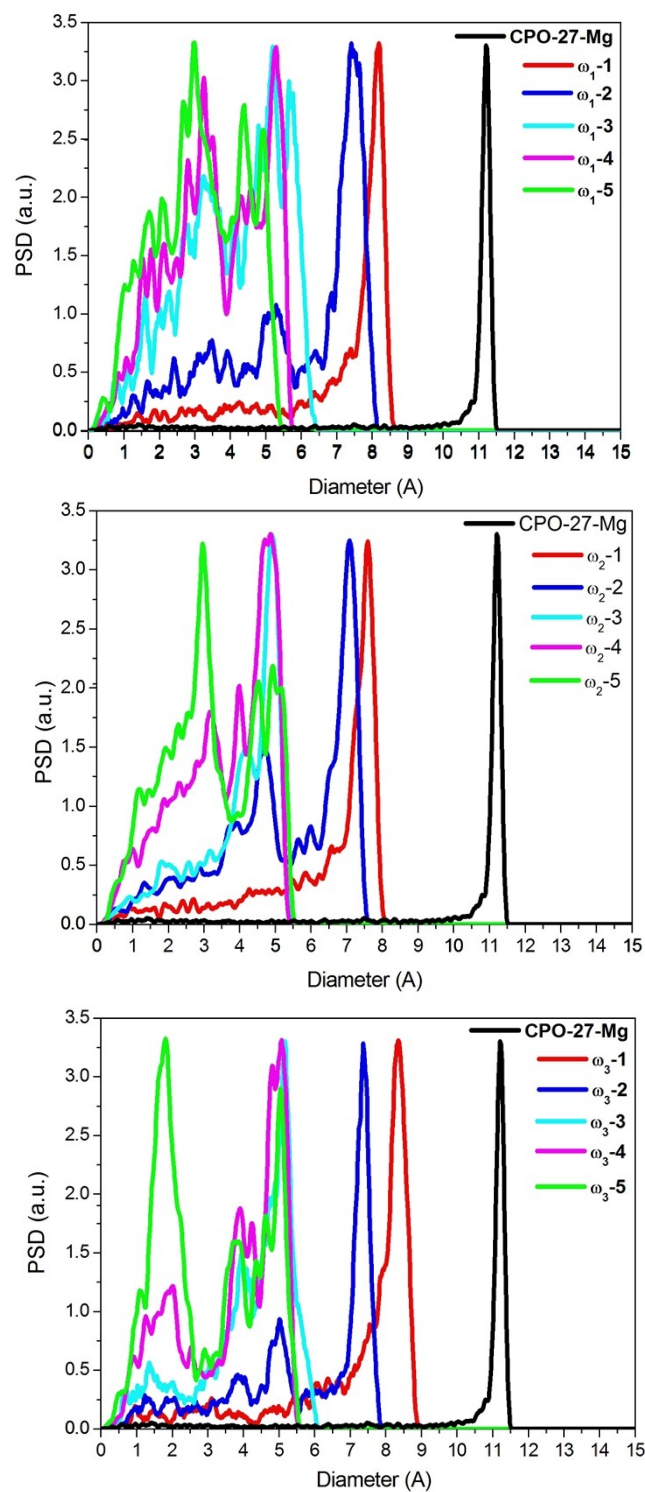


Figure S8. PSD of the structure of CPO-27-Mg and the corresponding to: ω_1 -J (up); ω_2 -J (middle) and ω_3 -J (bottom) models. The PSDs were normalized to compare with the non-functionalized material.

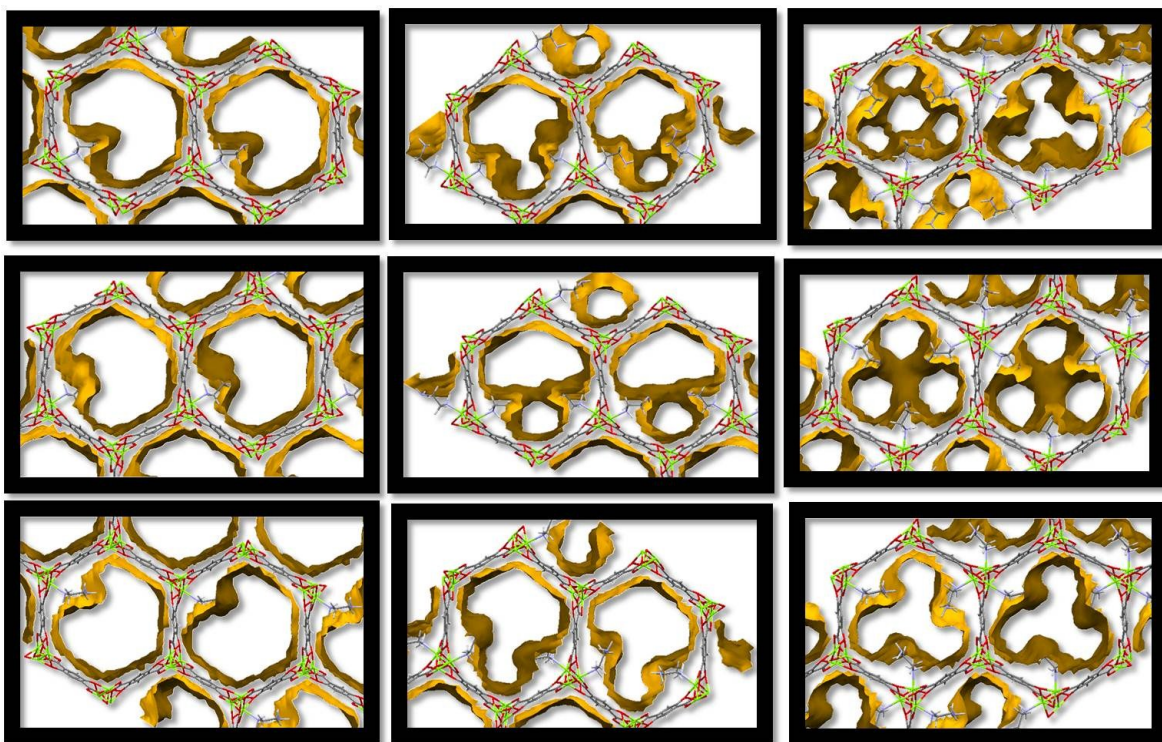


Figure S9. Projections of the structure of CPO-27-Mg corresponding to: ω_1 -1, ω_1 -2, ω_1 -3 (top); ω_2 -1, ω_2 -2, ω_2 -3 (middle) and ω_3 -1, ω_3 -2, ω_3 -3 (bottom) models, showing the contact surface (in yellow) of the resultant pore sub-structure.

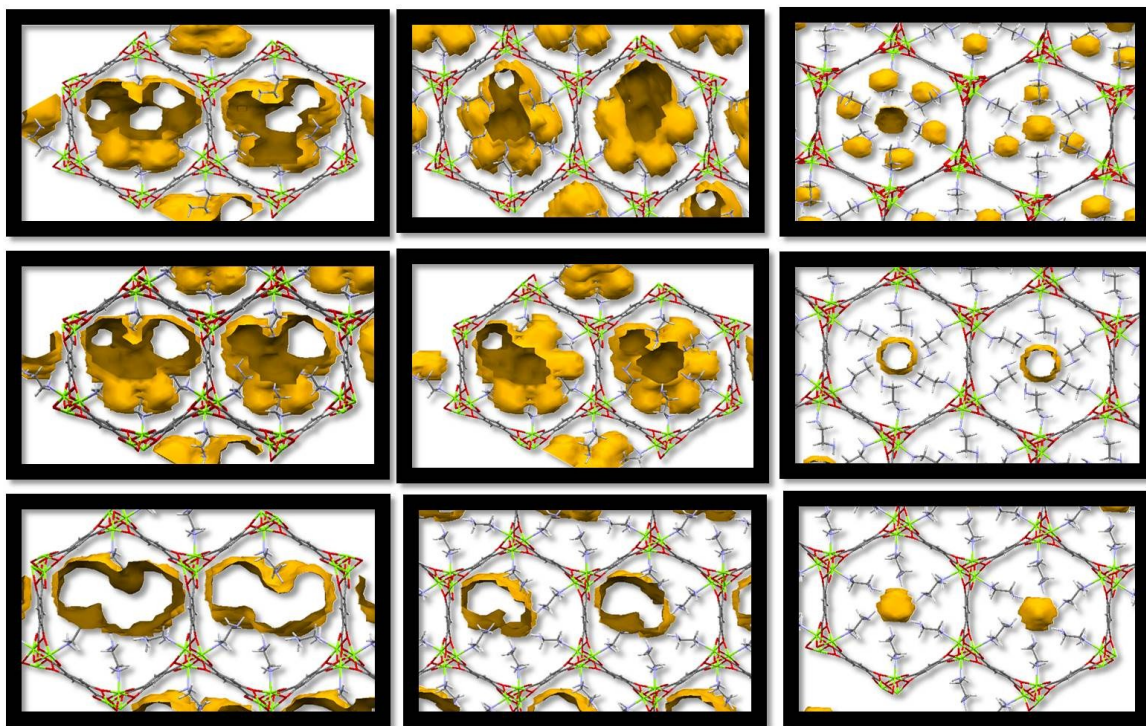


Figure S10. Projections of the structure of CPO-27-Mg corresponding to: ω_1 -4, ω_1 -5, ω_1 -6 (top); ω_2 -4, ω_2 -5, ω_2 -6 (middle) and ω_3 -4, ω_3 -5, ω_3 -6 (bottom) models, showing the contact surface (in yellow) of the resultant pore sub-structure.

Section S8. Forcefield and models information

LJ parameters for the C and O atoms of the **CPO-27** skeleton were taken from the DREIDING² force field and the corresponding to Mg atom was taken from the UFF³ force field; those parameters corresponding to C, H and N atoms belonging to the ethylenediamine portion were taken from the TraPPE force field⁴ developed for amine molecules. Partial charges for MOF atoms were derived from the partial equilibration procedure as implemented in the Forcite Module of Materials Studio. Table S3 shows the LJ parameters for all atom types found in the MOFs we investigated in this work.

Carbon dioxide was modeled as a linear triatomic molecule with fixed bond lengths and bond angles. The atoms were modeled by charged Lennard-Jones (LJ) centers using the TraPPE force field developed by Potoff and Siepmann.⁵ This force field has been fit to reproduce the vapor-liquid coexistence curves.

Table S2. Lennard-Jones parameters for framework atoms.

Atom type	$\sigma(\text{\AA})$	ϵ/k_B (K)	Force field
N_en	3.34	111.0	TraPPE
C_en	3.65	5.0	TraPPE
H_en	0.0	0.0	TraPPE
Mg_Mof	2.692	55.855	UFF
C_Mof	3.473	47.856	DREIDING
O_Mof	3.033	48.158	DREIDING

Table S3. LJ parameters and partial atomic charges for CO₂ atoms.

	C	O
$\sigma(\text{\AA})$	2.8	3.05
ϵ/k_B (K)	27	79.0
Q (e)	0.7	-0.35

Table S4. Dihedral angles of the ethylenediamine molecules grafted to CPO-27-Mg framework obtained after the energy minimization procedure

ω_1-1	ω_2-1	ω_3-1
68.22	62.45	176.62
ω_1-2	ω_2-2	ω_3-2
-66.63	68.34	177.27
-67.01	69.45	176.55
ω_1-3	ω_2-3	ω_3-3
-66.76	69.00	176.88
-66.76	69.01	176.88
-66.76	69.01	176.88
ω_1-4	ω_2-4	ω_3-4
-67.97	68.69	176.73
-68.27	83.31	-174.76
67.42	-68.22	176.68
-74.05	66.55	176.89
ω_1-5	ω_2-5	ω_3-5
-71.33	64.55	176.98
76.91	81.76	-175.90
-49.31	-70.93	175.77
65.76	67.16	-174.79
-69.92	63.54	175.79

¹ Dubbeldam, D.; Calero, S.; Ellis, D. E.; Snurr, R. Q. (2015): RASPA: molecular simulation software for adsorption and diffusion in flexible nanoporous materials, *Molecular Simulation*, DOI:10.1080/08927022.2015.1010082.

² Mayo, S. L.; Olafson, B. D.; Goddard, W. A. *J. Phys. Chem.* 1990, 94, 8897.

³ Rappe, A. K.; Casewit, C. J.; Colwell, K. S.; Goddard, W. A.; Skiff, W. M. *J. Am. Chem. Soc.* 1992, 114, 10024.

⁴ C. D. Wick, J. M. Stubbs, N. Rai, J. I. Siepmann *J. Phys. Chem. B* 2005, 109, 18974-18982.

⁵ a) Potoff, J. J.; Siepmann, J. I. *AIChE J.* 2001, 47, 1676; b) Martin, M. G.; Siepmann, J. I. *J. Phys. Chem. B* 1998, 102, 2569.